

# Pascal's Triangle Fractal Symmetries

Nayan E. Myerson-Jain,<sup>1</sup> Shang Liu,<sup>2</sup> Wenjie Ji,<sup>1</sup> Cenke Xu,<sup>1</sup> and Sagar Vijay<sup>1</sup>

<sup>1</sup>*Department of Physics, University of California, Santa Barbara, CA 93106, USA*

<sup>2</sup>*Kavli Institute for Theoretical Physics, University of California, Santa Barbara, CA 93106, USA*

We introduce a model of interacting bosons exhibiting an infinite collection of fractal symmetries – termed “Pascal’s triangle symmetries” – which provides a natural U(1) generalization of a spin-(1/2) system with Sierpinski triangle fractal symmetries introduced in Ref. [1]. The Pascal’s triangle symmetry gives rise to exact degeneracies, as well as a manifold of low-energy states which are absent in the Sierpinski triangle model. Breaking the U(1) symmetry of this model to  $Z_p$ , with prime integer  $p$ , yields a lattice model with a unique fractal symmetry which is generated by an operator supported on a fractal subsystem with Hausdorff dimension  $d_H = \ln(p(p+1)/2)/\ln p$ . The Hausdorff dimension of the fractal can be probed through correlation functions at finite temperature. The phase diagram of these models at zero temperature in the presence of quantum fluctuations, as well as the potential physical construction of the U(1) model are discussed.

PACS numbers:

*Introduction:* In recent years, generalizations of the notion of symmetry have significantly broadened our view on states of matter. Many previously developed phases, such as  $Z_2$  topological order [2–5], and the  $(3+1)d$  algebraic spin liquid with photon excitations [6–8], were thought to be beyond the notion of spontaneous symmetry breaking (SSB) of ordinary global symmetries. But it has been realized in recent years that these phases still have a unified description as the SSB of generalized higher-form symmetries [9–17]. The notion of subsystem symmetry has further enriched our understanding along this line. Long-range-entangled quantum phases with fractionalized excitations that exhibit restricted mobility – termed fracton orders – exhibit emergent subsystem symmetries [18–22]. Subsystem symmetries can be categorized into type-I and II [18], where a type-I subsystem symmetry has generators and conserved charges defined on regular submanifolds of the system, such as lines and planes, while type-II subsystem symmetries have conserved charges defined on a fractal-shaped subsystem [20, 23], often with non-integer spatial dimensions.

The simplest model with a fractal subsystem symmetry is the Sierpinski-triangle model, which was first introduced for the purpose of studying glassy dynamics in the absence of disorder [1]:

$$H_{\text{ST}} = \sum_{\nabla} -K \sigma_1^z \sigma_2^z \sigma_3^z. \quad (1)$$

Here  $\sigma_i^z$  is an Ising spin defined on each site of a triangular lattice, and the sum is only over the downward-facing triangular plaquettes of the lattice. This simple model has the following desirable features. (1) The model has an exotic “fractal symmetry”, which becomes most explicit when the system is defined on a  $L \times L$  lattice with  $L = 2^k - 1$ : the Hamiltonian is invariant under flipping spins on a Sierpinski-triangle fractal subsystem; (2) at finite temperature, the three point correlation function  $\langle \sigma_{0,0}^z \sigma_{r,0}^z \sigma_{0,r}^z \rangle$  is nonzero only when  $r = 2^k$ , and scales as

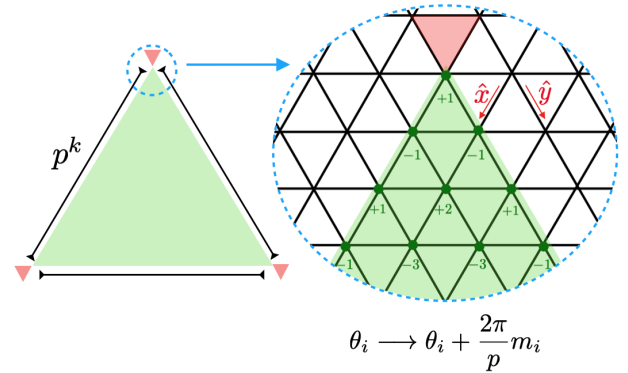


**FIG. 1: Pascal’s Triangle Symmetries:** The U(1) parent model (2) has a family of fractal symmetries, generated by a staggered rotation of the boson phase  $\theta_i \rightarrow \theta_i + \frac{2\pi}{p} m_i$  over a triangular region of side length which is a power of any prime number  $p$ . For each  $p$ , the fractal symmetry becomes exact for system size  $L^2$  with  $L = p^k - 1$ . When acting on a classical ground-state of the parent model, this transformation generates excitations at the corners of the triangular region. The non-trivial action of this rotation can be visualized as Pascal’s triangle modulo  $p$ , which is a fractal with Hausdorff dimension  $d_H(p) = \ln(p(p+1)/2)/\ln p$ .

$\sim \exp(-r^{d_H})$  with  $d_H = \ln 3/\ln 2$ , which is the Hausdorff dimension of the Sierpinski-triangle [23]; (3) with a transverse field  $\sum_i -h \sigma_i^x$ , the system becomes a quantum Sierpinski-triangle model, and at  $h = K$  there is a quantum phase transition at zero temperature [24, 25], which separates the “fractal-ordered” phase that spontaneously breaks the fractal symmetry ( $K > h$ ), and a disordered phase with ( $h > K$ ).

In this work we introduce generalizations of both the classical and quantum Sierpinski-triangle models. These models are obtained from a U(1) parent model with “Pascal’s triangle” (also called Yang Hui triangle in China) symmetries, a family of symmetry transformations along a fractal region which are exact in a system with pe-

riodic boundary conditions, and for particular system sizes. Even when these symmetries are not exact, the presence of an “approximate” Pascal’s triangle symmetry gives rise to low-energy states which are absent in the Sierpinski triangle model [1]. Descendant models are obtained by reducing the U(1) degree of freedom of the parent model to  $Z_p$ , with prime integer  $p$ . The  $Z_p$  models have their own fractal symmetry that are deduced from the Pascal’s triangle symmetry, and their degenerate excitations have an emergent fractal structure with Hausdorff dimension  $d_H = \ln(p(p+1)/2)/\ln p$ .

*The U(1) parent model:* The Hamiltonian of the U(1) generalization of the Sierpinski-triangle model reads

$$H_{U(1)} = \sum_{\nabla} -t \cos(\theta_1 + \theta_2 + \theta_3). \quad (2)$$

It is straightforward to see that Eq. 2 has two conventional U(1) global symmetries:

$$\begin{aligned} U(1)_1 : \theta_{j \in A} &\rightarrow \theta_{j \in A} + \alpha, & \theta_{j \in B} &\rightarrow \theta_{j \in B} - \alpha, \\ U(1)_2 : \theta_{j \in A} &\rightarrow \theta_{j \in A} + \beta, & \theta_{j \in C} &\rightarrow \theta_{j \in C} - \beta. \end{aligned} \quad (3)$$

$A, B, C$  are the three sublattices of the triangular lattice. The ground states of Eq. 2 spontaneously break the two U(1) symmetries. Starting with one of the ground states, say  $\theta = 0$  uniformly on the entire lattice, a class of ground states can be generated by rotating  $\theta$  globally according to Eq. 3. Any ground state obtained this way still has a uniform order of  $\theta$  on each of the three sublattices, hence the ground states generated through Eq. 3 have a conventional “ $\sqrt{3} \times \sqrt{3}$ ” order, which is the order often observed on the triangular lattice antiferromagnet.

Besides the two ordinary U(1) global symmetries, this model Eq. 2 actually contains an infinite series of  $Z_p$  distinct fractal symmetries, one for each prime number  $p$ ,  $p \geq 2$ . In contrast to the classical Sierpinski-triangle model, where the  $Z_2$  fractal subsystem symmetry is taken as a sequence of spin flips in the shape of a Sierpinski-triangle, the series of  $Z_p$  fractal symmetries exhibited by the U(1) parent model are in the shape of a Pascal’s triangle modulo  $p$ . For example when  $p = 2$ , this Pascal’s triangle symmetry reduces down to the familiar  $Z_2$  fractal symmetry of the Sierpinski-triangle model; for  $p = 3$  the Pascal’s triangle modulo 3 reduces to another fractal shape (Fig. 1).

The exact series of fractal transformations of Eq. 2 can be written down as a staggered rotation of the  $\theta_i$ ’s in the shape of a Pascal’s triangle modulo  $p$ , which has a side-length of  $p^k - 1$ , where  $k$  is any integer greater than zero. The precise form of the transformation is

$$\theta_i \longrightarrow \theta_i + \frac{2\pi}{p} (-1)^{i_x + i_y} \begin{pmatrix} i_x + i_y \\ i_y \end{pmatrix}. \quad (4)$$

at the points  $(i_x, i_y)$  for which  $0 \leq i_y \leq i_x$  and  $i_x + i_y \in [0, p^k - 1]$ . As shown in the Supplemental Material

(SM), transformations of this form can be used to generate exact symmetries when the system is placed on an  $L \times L$  lattice with periodic boundary conditions and with  $L = p^k - 1$ .

Any  $Z_p$  fractal transformation of the U(1) parent model which is not an exact symmetry of the model generates fully immobile defects which are analogous to fractons. From the uniform  $\theta_i = 0$  ground-state, transforming the U(1) degrees of freedom according to Eq. 4 in the shape of a local Pascal’s triangle of size  $p^k - 1$  creates three defects of energy  $t(1 - \cos(2\pi/p))$ , one at each downward-facing triangular plaquette located at the corners of the Pascal’s triangle, as shown in the SM, and as indicated schematically in Fig. 1. If we treat these defects as point-like quasiparticles localized on their downward facing plaquettes, individual defects cannot be moved by any rotation of  $\theta_i$ ’s without creating more excitations and are hence completely immobile. We note that since  $p$  can be arbitrarily large, the excitations created by a  $Z_p$  fractal transformation can cost a vanishingly small energy in a thermodynamically large system.

At finite temperature, the U(1) parent model is completely disordered similarly to the Sierpinski-triangle model [1]. This can be most easily seen from a duality mapping of the U(1) degrees of freedom on the vertices to new U(1) degrees of freedom on downward facing plaquettes  $(\theta_1 + \theta_2 + \theta_3)_{\nabla} \rightarrow \phi_{\nabla}$ , where  $\phi_{\nabla}$  is defined on the dual site located at the center of each downward facing triangular plaquette (Fig. 2), and  $\phi$  is still compact (periodically defined). The dual of the U(1) parent model is

$$H_{U(1)}^d = \sum_{\nabla} -t \cos(\phi_{\nabla}). \quad (5)$$

Since each  $\phi$  is decoupled from one another, the partition function factorizes into a product of local partition functions for each individual  $\phi$  which does not support any phase transition.

The three-body interactions of the Sierpinski-triangle model, as well as the U(1) parent model look artificial. Ref. [26] proposed to realize the Sierpinski-triangle model with the Rydberg atoms with only two-body Van der Waals interactions. In the SM we present a more natural construction of the U(1) parent model through a set-up with only two-body interactions.

*The  $Z_p$  models:* From the U(1) parent model Eq. 2, models with a single fractal symmetry that are natural extensions of the Sierpinski-triangle model can be constructed. This is done by breaking the U(1) degrees of freedom down to  $Z_p$  clock degrees of freedom  $\sigma_i = e^{i\theta_i}$ ,  $\theta_i \in \frac{2\pi}{p} Z_p$ :

$$H_{Z_p} = \sum_{\nabla} -\frac{t}{2} \sigma_1 \sigma_2 \sigma_3 + \text{h.c.} \quad (6)$$

The model Eq. 6 extends many properties of the Sierpinski-triangle model to a more general series of  $Z_p$

“Pascal’s triangle models” which reduces to Eq. 1 when  $p = 2$ . Generally, since the  $Z_p$  fractal symmetry of the Pascal’s triangle models are descended from the  $U(1)$  parent model, the fractal symmetry transformation in these models is realized by Eq. 4 with the appropriate choice of  $p$ . These series of models also display the fracton-like defects associated to fractal excitations in the shape of a Pascal’s triangle modulo  $p$  that cost energy  $t(1 - \cos(\frac{2\pi}{p}))$  each as well as spontaneously breaking the  $Z_p$  fractal symmetry, yielding a ground-state degeneracy of  $p^{L-1}$  when  $L = p^k - 1$  (see SM for derivation).

Spontaneous symmetry breaking of the  $Z_p$  fractal symmetries in the Pascal’s triangle models can be diagnosed by the behavior of a three-point correlation function. Making use of the duality of these models, we can define plaquette degrees of freedom  $\tau_{\nabla} = (\sigma_1\sigma_2\sigma_3)_{\nabla}$ . The dual Hamiltonian is

$$H_{Z_p}^d = \sum_{\nabla} -\frac{t}{2}\tau_{\nabla} + \text{h.c.} \quad (7)$$

In the thermodynamic limit, each  $\sigma$ -variable can be represented as an infinite staggered product of dual  $\tau$ -variables in the shape of a Pascal’s triangle modulo  $p$ . The three-point function  $\mathcal{C}_3(r) = \langle \sigma_{0,0}\sigma_{r,0}\sigma_{0,r} \rangle$ , after being rewritten in terms of the dual variables only has compact support when  $r = p^k$  and hence must vanish else wise. The three-point function factors into a product of single-site expectation values  $\langle \tau \rangle, \dots, \langle \tau^{p-1} \rangle$ . From the form of the Hamiltonian, a general expression for the three-point function for arbitrary  $p$  prime can be derived (see SM for details)

$$\mathcal{C}_3(r = p^k) = \prod_{m=1}^{\frac{p-1}{2}} \langle \tau^m \rangle^{N_{m,p-m}(k)}, \quad (8)$$

$N_{m,p-m}(k)$  is the number of times  $m$  and  $p-m$  appear in a Pascal’s triangle modulo  $p$  with length  $p^k - 1$ . Such an expression is complex, but a complete set of recurrence relations is constructed in the SM for  $N_{m,p-m}(k)$  lending Eq. 8 to efficient numerical evaluation. For small  $p$  this can be done analytically, e.g. for  $p = 3$ , the three-point function is

$$\begin{aligned} \mathcal{C}_3(r = 3^k) &= \langle \tau \rangle^{r^{d_H}} \\ &= \left( \frac{e^{\beta t} - e^{-\beta t/2}}{e^{\beta t} + 2e^{-\beta t/2}} \right)^{r^{d_H}} \sim e^{-\alpha r^{d_H}}, \end{aligned} \quad (9)$$

where  $d_H = \frac{\ln 6}{\ln 3}$  is the Hausdorff dimension of a Pascal’s triangle modulo 3. In general there are natural bounds on the decay of the three-point function:  $\mathcal{C}_3(r = p^k)$  will decay hyper-exponentially as  $\sim e^{-\alpha r^\gamma}$  for sufficiently large  $r$ , where the exponent of the decay  $\gamma$  is bounded such that

$$d_H \leq \gamma \leq \left( \frac{p-1}{2} \right) d_H, \quad p > 2. \quad (10)$$

As demonstrated by Eqs. 8 and 10, the decay of the three-point function can be complicated for general  $p$  prime. However, a modified version of the  $Z_p$  Pascal’s triangle models in Eq. 6 can be proposed for which the three-point function at finite temperature always decays as a fractal area-law. If we consider an equal-weight summation of plaquette terms

$$\mathcal{H}_p = \sum_{\nabla} \sum_{m=0}^{\frac{p-1}{2}} -\frac{t}{2}(\sigma_1\sigma_2\sigma_3)^m + \text{h.c.} \quad (11)$$

This model retains the  $Z_p$  fractal symmetry of Eq. 6 as it only includes products of the original plaquette terms. As such, the duality  $(\sigma_1\sigma_2\sigma_3)_{\nabla} \rightarrow \tau_{\nabla}$  still exists and the dual of  $\mathcal{H}_p$  is

$$\mathcal{H}_p^d = \sum_{\nabla} \sum_{m=0}^{\frac{p-1}{2}} -\frac{t}{2}\tau_{\nabla}^m + \text{h.c.} \quad (12)$$

The manner in which the three-point correlation for  $\mathcal{H}_p$  is calculated remains the same as for what it was in Eq. 6 with the exception that  $\langle \tau^m \rangle$  no longer depends on power,  $m$ . As a result,  $\mathcal{C}_3(r = p^k)$  decays as a fractal area-law no matter what value  $p$  takes:

$$\begin{aligned} \mathcal{C}_3(r = p^k) &= \langle \tau \rangle^{r^{d_H}}, \\ &= \left( \frac{e^{(\frac{p+1}{2})\beta t} - e^{\frac{\beta t}{2}}}{e^{(\frac{p+1}{2})\beta t} + (p-1)e^{\frac{\beta t}{2}}} \right)^{r^{d_H}} \sim e^{-\alpha r^{d_H}}. \end{aligned} \quad (13)$$

The  $Z_p$  Pascal’s triangle model with prime integer  $p$  can be further extended to  $Z_N$  models where  $N$  is a composite positive integer. These new composite  $Z_N$  models have more than one fractal symmetry. In fact, there is a distinct  $Z_p$  fractal symmetry for each unique prime divisor of  $N$ , e.g. the  $Z_{N=6}$  model has a  $Z_2$  Sierpinski-triangle fractal symmetry and a  $Z_3$  Pascal’s triangle modulo 3 fractal symmetry. The behavior of the three-point correlations of the  $Z_N$  models is further discussed in the SM.

*The Quantum Phase diagram:* So far we have only discussed the classical version of the models. To turn quantum fluctuations on in Eq. 2, one can modify the model as

$$H_{Q-U(1)} = \sum_{\nabla} -t \cos(\theta_1 + \theta_2 + \theta_3) + \sum_j \frac{U}{2} n_j^2, \quad (14)$$

where  $n_j$  is the boson number operator defined on each site of the triangular lattice, which are conjugate to the boson phase  $[n_i, \theta_j] = i\delta_{ij}$ .

As shown previously, a class of ground states of the classical  $U(1)$  model Eq. 2 have the conventional  $\sqrt{3} \times \sqrt{3}$  order, which spontaneously breaks the Pascal’s triangle symmetry, and the two  $U(1)$  symmetries in Eq. 3.

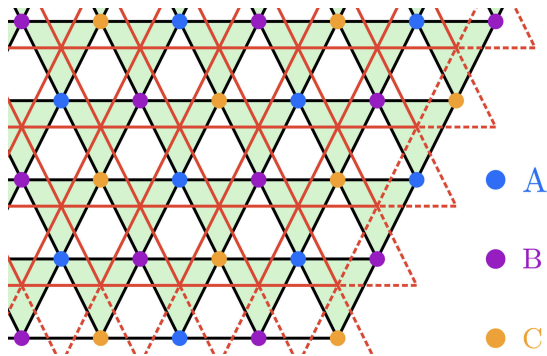


FIG. 2: **The U(1) Model and its Dual Description:** The models we consider in this work involve sum of all the downward facing triangles (shaded in green); The dual of the U(1) model (Eq. 5, Eq. 17) is defined on the dual triangular lattice, whose sites are the center of each downward facing triangles of the original lattice.

We now investigate whether this classical order is stable against quantum fluctuation, i.e. whether it is stable against the  $U$  term in Eq. 14. We argue that all symmetries of the Hamiltonian (14) are restored by quantum fluctuations.

In an ordered phase that spontaneously breaks the U(1) global symmetry, one can ignore the fact that the phase angle  $\theta$  is a compact boson (i.e.  $\theta \sim \theta + 2\pi$ ), and hence expand the cosine function of Eq. 14 to the lowest nontrivial order. This procedure leads to an approximate Gaussian Hamiltonian:

$$H_{Q-U(1)}^g = \sum_{i,j} t\theta_i\theta_j + \sum_j 3t\theta_j^2 + \frac{U}{2}n_j^2. \quad (15)$$

The band structure of  $\theta$  based on this Gaussian Hamiltonian has minima at  $\pm\mathbf{K} = \pm(4\pi/3, 0)$ , which is consistent with the  $\sqrt{3} \times \sqrt{3}$  order of the classical Hamiltonian. The spectrum of the Gaussian Hamiltonian is gapless.

The Gaussian expansion of the Hamiltonian ignored the compactness of  $\theta$ . In a quantum model constructed with  $\theta$ ,  $\theta$  being a compact boson is equivalent to the constraint that its quantum conjugate variable  $n$  take discrete values. To check the stability of a semiclassical state of  $\theta$  under quantum fluctuation, one needs to investigate whether the compactness of  $\theta$ , or equivalently the discrete nature of  $n$  would destabilize the semiclassical state described by the Gaussian Hamiltonian Eq. 15. For example, the  $(2+1)d$  quantum dimer model on the square lattice can be mapped to a compact U(1) gauge theory [27, 28], a Gaussian expansion would lead to gapless photons. But the compactness of the gauge field is always relevant in a semiclassical photon state unless the system is at a fine-tuned multicritical point (the so-called RK point [27]), hence the Gaussian state is generally unstable against quantum fluctuations. This effect is also referred to as confinement of a lattice gauge theory. The

standard method of the analysis relies on the dual formalism of Eq. 14 and Eq. 15. The dual model is defined on the dual triangular lattice (Fig. 2), by introducing the following variables:

$$\sum_{j \in \nabla} \theta_j = \phi_{\bar{j}}, \quad n_j = \sum_{\bar{j} \in \Delta \text{ around } j} \Psi_{\bar{j}}. \quad (16)$$

where  $\bar{j}$  denotes the sites of the dual triangular lattice.  $\phi_{\bar{j}}$  and  $\Psi_{\bar{j}}$  are canonically conjugate variables.  $\Psi_{\bar{j}}$  takes half-integer values, and  $\phi_{\bar{j}}$  is compact. The dual Hamiltonian reads

$$H_{Q-U(1)}^d = \sum_{\bar{j}} -t \cos(\phi_{\bar{j}}) + \sum_{\bar{\Delta}} \frac{U}{2} (\Psi_{\bar{1}} + \Psi_{\bar{2}} + \Psi_{\bar{3}})^2 \quad (17)$$

Instead of directly dealing with the discrete variable  $\Psi$ , we may view  $\Psi_{\bar{j}}$  as taking continuous values, and  $\phi_{\bar{j}}$  as its non-compact conjugate variable. The discrete nature of  $\Psi$  can be enforced through an external potential in the dual Hamiltonian. The dual Hamiltonian becomes

$$H_{Q-U(1)}^d \sim \sum_{\bar{\Delta}} \frac{U}{2} (\Psi_{\bar{1}} + \Psi_{\bar{2}} + \Psi_{\bar{3}})^2 - \sum_{\bar{j}} t \cos(\phi_{\bar{j}}) - \alpha \cos(2\pi\Psi_{\bar{j}}). \quad (18)$$

The next step is to temporarily ignore the  $\alpha$ -terms, and expand  $-t \cos(\phi_{\bar{j}})$  to the lowest nontrivial order. After this procedure, the dual Hamiltonian takes a Gaussian form, and it is the dual of the Gaussian Hamiltonian Eq. 15. The goal of this analysis is to check the role of the  $\alpha$ -terms at this Gaussian state. This dual Gaussian Hamiltonian can be solved, leading to a band structure of  $\Psi$ . The minima of the band structure of  $\Psi$  are located at the two corners of the Brillouin zone,  $\pm\mathbf{K} = (\pm 4\pi/3, 0)$ . We then expand  $\Psi_{\mathbf{r}}$  at  $\pm\mathbf{K}$ :

$$\Psi(\mathbf{r}) \sim e^{i\mathbf{K} \cdot \mathbf{r}} \psi(\mathbf{r}) + e^{-i\mathbf{K} \cdot \mathbf{r}} \psi^*(\mathbf{r}). \quad (19)$$

The Lagrangian of the dual theory expanded at  $\pm\mathbf{K}$  becomes

$$\mathcal{L}_{Q-U(1)}^d = (\partial_\tau \vec{\psi})^2 + \rho_2 (\nabla \vec{\psi})^2 - \sum_a \alpha \cos(\vec{e}_a \cdot \vec{\psi}), \quad (20)$$

where  $\vec{\psi} = (\text{Re}(\psi), \text{Im}(\psi))$ ;  $a = A, B, C$  label the three sublattices of the dual triangular lattice, and  $e_A = 2\pi(1, 0)$ ,  $e_B = 2\pi(-1/2, \sqrt{3}/2)$ ,  $e_C = 2\pi(-1/2, -\sqrt{3}/2)$ .

The last three terms in Eq. 20 arise from rewriting the last term of Eq. 18 by expanding  $\Psi$  at  $\pm\mathbf{K}$ . After this expansion, the last term of Eq. 18 becomes  $-\alpha \cos(\vec{e}_a \cdot \vec{\psi}(\mathbf{r}))$  for  $\mathbf{r}$  belonging to sublattice  $a$  ( $a = A, B, C$ ) of the dual triangular lattice. Hence at long scale a nonvanishing term would survive. The  $\alpha$  term in Eq. 20 will be relevant for the Gaussian theory with nonzero  $\rho_2$ , which implies that the compactness of  $\theta$ , or the discrete nature of  $n$  in Eq. 14 destabilizes the semiclassical Gaussian state,



and the spectrum of Eq. 14 should be gapped even with small  $U$ .

The dual description of the U(1) model studied here accurately captures the spectrum of the gapless modes arising from spontaneously breaking the global U(1) symmetries, though it does not reproduce the spectrum at  $U = 0$  that arise due to the Pascal triangle symmetries. Nevertheless, the nature of the ground-state of the system when the pinning potential flows to strong coupling can still be inferred. A strong  $\alpha$  would pin  $\Psi$  to integer values, which implies that a relevant  $\alpha$  would drive the system into an eigenstate of  $n$  in Eq. 14, and the  $U$  term will lead to a unique and gapped ground state without any spontaneous symmetry breaking. Hence we postulate that quantum fluctuations of Eq. 14 restores all the symmetries of model Eq. 2, and continuously connects to the large- $U$  limit of Eq. 14. The analysis here would be more involved if  $n$  takes half integer values in Eq. 14.

One possible quantum generalization of Eq. 6 is

$$H_{Q-Z_p} = \sum_{\nabla} -t\sigma_1^z\sigma_2^z\sigma_3^z - \sum_j h\sigma_j^x + \text{h.c.} \quad (21)$$

for which the clock operators  $\sigma^z$  and  $\sigma^x$  obey  $(\sigma^z)^p = (\sigma^x)^p = 1$  and  $\sigma^z\sigma^x = e^{2\pi i/p}\sigma^x\sigma^z$  (one can also take  $\sigma^z = \exp(i\theta)$  and  $\sigma^x = \exp(i2\pi n/p)$ , and restrict  $\theta$  to take values in  $\frac{2\pi}{p}Z_p$ ). Unlike the quantum U(1) model, Eq. 21 is exactly self-dual with the introduction of the dual plaquette variables

$$\tau_j^x = \sigma_1^z\sigma_2^z\sigma_3^z, \quad \tau_1^z\tau_2^z\tau_3^z = \sigma_j^x \quad (22)$$

for which the dual Hamiltonian takes the same form as Eq. 21 with  $t$  and  $h$  switched. Since the spectrum of the  $Z_p$  models at  $h = 0$  is gapped, and it takes infinite order of perturbations of  $h$  to mix two different ground states in the thermodynamics limit, the classical fractal-order of the  $Z_p$  Pascal's triangle models is not destroyed upon the introduction of quantum fluctuations. Furthermore, the exact self-duality implies that there should be one or more quantum phase transitions that separate the fractal ordered phase ( $t \gg h$ ) and the disordered phase ( $h \gg t$ ).

*Discussion:* Although we demonstrated that the semiclassical order of Eq. 14 is unstable against quantum fluctuation, some deformation of Eq. 14 can support a stable semiclassical order. In the SM we will show that if we sum over three-boson interactions for both upward-facing and downward-facing triangles, the semiclassical  $\sqrt{3} \times \sqrt{3}$  order becomes stable against quantum fluctuations. Also, the system may be tuned to a multicritical point where  $\rho_2$  in Eq. 20 vanishes, and the low energy dynamics is controlled by  $\rho_4(\nabla^2\psi)^2$ . The system can remain gapless for a finite range of  $\rho_4$ , though it takes tuning multiple parameters to reach this state [29–31].

The nature of the quantum phase transition(s) in the quantum  $Z_p$  model is a challenging subject. So far there is no well established paradigm for understanding quantum phase transitions involving spontaneous breaking of

a fractal symmetry. Any approach to study the quantum phase transition of the  $Z_p$  models (such as the quantum  $Z_2$  Sierpinski-triangle model) through the U(1) generalization would need to address the enlarged Pascal's triangle symmetry pointed out in the current work.

C.X. is supported by NSF Grant No. DMR-1920434, and the Simons Investigator program.

- 
- [1] M. E. J. Newman and C. Moore, Phys. Rev. E **60**, 5068 (1999), URL <https://link.aps.org/doi/10.1103/PhysRevE.60.5068>.
- [2] N. Read and S. Sachdev, Phys. Rev. Lett. **66**, 1773 (1991), URL <https://link.aps.org/doi/10.1103/PhysRevLett.66.1773>.
- [3] X. G. Wen, Phys. Rev. B **44**, 2664 (1991), URL <https://link.aps.org/doi/10.1103/PhysRevB.44.2664>.
- [4] R. Moessner and S. L. Sondhi, Phys. Rev. Lett. **86**, 1881 (2001), URL <https://link.aps.org/doi/10.1103/PhysRevLett.86.1881>.
- [5] A. Kitaev, Annals of Physics **303**, 2 (2003), ISSN 0003-4916, URL <https://www.sciencedirect.com/science/article/pii/S0003491602000180>.
- [6] X.-G. Wen, Phys. Rev. B **68**, 115413 (2003), URL <https://link.aps.org/doi/10.1103/PhysRevB.68.115413>.
- [7] R. Moessner and S. L. Sondhi, Phys. Rev. B **68**, 184512 (2003), URL <https://link.aps.org/doi/10.1103/PhysRevB.68.184512>.
- [8] M. Hermele, M. P. A. Fisher, and L. Balents, Phys. Rev. B **69**, 064404 (2004), URL <https://link.aps.org/doi/10.1103/PhysRevB.69.064404>.
- [9] Z. Nussinov and G. Ortiz, Annals of Physics **324**, 977 (2009), ISSN 0003-4916, URL <http://dx.doi.org/10.1016/j.aop.2008.11.002>.
- [10] O. Aharony, N. Seiberg, and Y. Tachikawa, Journal of High Energy Physics **2013** (2013), ISSN 1029-8479, URL [http://dx.doi.org/10.1007/JHEP08\(2013\)115](http://dx.doi.org/10.1007/JHEP08(2013)115).
- [11] S. Gukov and A. Kapustin (2013), 1307.4793.
- [12] A. Kapustin and R. Thorngren (2013), 1308.2926.
- [13] A. Kapustin and R. Thorngren (2013), 1309.4721.
- [14] A. Kapustin and N. Seiberg, Journal of High Energy Physics **2014** (2014), ISSN 1029-8479, URL [http://dx.doi.org/10.1007/JHEP04\(2014\)001](http://dx.doi.org/10.1007/JHEP04(2014)001).
- [15] D. Gaiotto, A. Kapustin, N. Seiberg, and B. Willett, Journal of High Energy Physics **2015** (2015), ISSN 1029-8479, URL [http://dx.doi.org/10.1007/JHEP02\(2015\)172](http://dx.doi.org/10.1007/JHEP02(2015)172).
- [16] P.-S. Hsin, H. T. Lam, and N. Seiberg, SciPost Physics **6** (2019), ISSN 2542-4653, URL <http://dx.doi.org/10.21468/SciPostPhys.6.3.039>.
- [17] C. Córdova, T. T. Dumitrescu, and K. Intriligator, Journal of High Energy Physics **2019**, 184 (2019), 1802.04790.
- [18] S. Vijay, J. Haah, and L. Fu, Phys. Rev. B **94**, 235157 (2016), URL <https://link.aps.org/doi/10.1103/PhysRevB.94.235157>.
- [19] S. Vijay, J. Haah, and L. Fu, Phys. Rev. B **92**, 235136 (2015), URL <https://link.aps.org/doi/10.1103/PhysRevB.92.235136>.
- [20] J. Haah, Phys. Rev. A **83**, 042330 (2011), URL <https://link.aps.org/doi/10.1103/PhysRevA.83.042330>.

- [21] R. M. Nandkishore and M. Hermele, Annual Review of Condensed Matter Physics **10**, 295 (2019), <https://doi.org/10.1146/annurev-conmatphys-031218-013604>, URL <https://doi.org/10.1146/annurev-conmatphys-031218-013604>.
- [22] M. Pretko, X. Chen, and Y. You, International Journal of Modern Physics A **35**, 2030003 (2020), <https://doi.org/10.1142/S0217751X20300033>, URL <https://doi.org/10.1142/S0217751X20300033>.
- [23] B. Yoshida, Phys. Rev. B **88**, 125122 (2013), URL <https://link.aps.org/doi/10.1103/PhysRevB.88.125122>.
- [24] L. M. Vasiloiu, T. H. E. Oakes, F. Carollo, and J. P. Garahan, Phys. Rev. E **101**, 042115 (2020), URL <https://link.aps.org/doi/10.1103/PhysRevE.101.042115>.
- [25] Z. Zhou, X.-F. Zhang, F. Pollmann, and Y. You (2021), 2105.05851.
- [26] N. E. Myerson-Jain, S. Yan, D. Weld, and C. Xu (2021), 2108.07765.
- [27] D. S. Rokhsar and S. A. Kivelson, Phys. Rev. Lett. **61**, 2376 (1988), URL <https://link.aps.org/doi/10.1103/PhysRevLett.61.2376>.
- [28] E. FRADKIN and S. KIVELSON, Modern Physics Letters B **04**, 225 (1990), <https://doi.org/10.1142/S0217984990000295>, URL <https://doi.org/10.1142/S0217984990000295>.
- [29] E. Fradkin, D. A. Huse, R. Moessner, V. Oganesyan, and S. L. Sondhi, Phys. Rev. B **69**, 224415 (2004), URL <https://link.aps.org/doi/10.1103/PhysRevB.69.224415>.
- [30] E. Ardonne, P. Fendley, and E. Fradkin, Annals of Physics **310**, 493 (2004), ISSN 0003-4916, URL <https://www.sciencedirect.com/science/article/pii/S0003491604000247>.
- [31] A. Vishwanath, L. Balents, and T. Senthil, Phys. Rev. B **69**, 224416 (2004), URL <https://link.aps.org/doi/10.1103/PhysRevB.69.224416>.
- [32] C. Xu and A. Vishwanath (2006), unpublished.

### Construction of the U(1) parent model

The three-body interaction of the U(1) parent model is artificial because the nature is dominated by two-body interactions. In what follows, we will discuss a more natural construction of the U(1) model through a set-up with only two-body interactions. The microscopic system we start with is a honeycomb lattice, with a spin-3/2 degree of freedom  $\vec{S}_R$  on each site  $R$  of sublattice  $\mathcal{A}$  of the honeycomb lattice, and a spin-1/2 degree of freedom  $\vec{s}$  on each site of sublattice  $\mathcal{B}$ . The initial model only has two body interactions:

$$\begin{aligned} H_0 &= \sum_{R \in \mathcal{A}} \sum_{b=1}^3 J \left( S_R^x s_{R,b}^x + S_R^y s_{R,b}^y \right) - D (S_R^z)^2 \\ &= \sum_{R \in \mathcal{A}} \sum_{b=1}^3 \frac{J}{2} \left( S_R^+ s_{R,b}^- + S_R^- s_{R,b}^+ \right) - D (S_R^z)^2 \end{aligned} \quad (23)$$

The first sum of  $R$  is over all the sites on sublattice  $\mathcal{A}$ , the second sum  $\sum_{b=1}^3$  is over the three neighboring sites

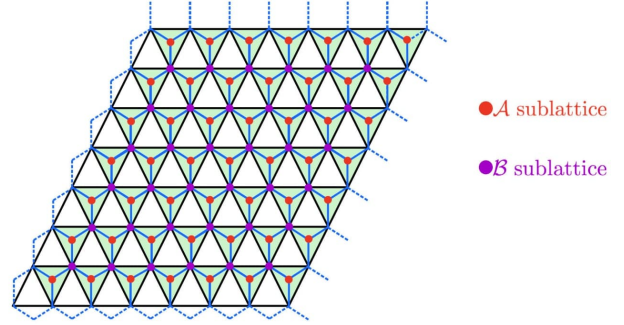


FIG. 3: The honeycomb lattice where Eq. 23 is defined on. The sublattice  $\mathcal{B}$  of the honeycomb lattice coincides with the sites of the triangular lattice of Eq. 1 and Eq. 2.

on sublattice  $\mathcal{B}$  around  $R$ . We also consider other interactions between second-neighbor sites, or equivalently first-neighbor sites within respective sublattices  $\mathcal{A}$  and  $\mathcal{B}$ :

$$H' = \sum_{R, R' \in \mathcal{A}} J_1 (S_R^x S_{R'}^x + S_R^y S_{R'}^y) + \sum_{i, j \in \mathcal{B}} J_2 (s_i^x s_j^x + s_i^y s_j^y) \quad (24)$$

The  $D$  term in Eq. 23 is an onsite spin anisotropy term. If  $D$  is positive and large, at low energy only the process that tunnels between  $S^z = -3/2$  and  $S^z = +3/2$  is allowed. At the third order perturbation of  $J$ , a nontrivial term is generated within the low energy Hilbert space, which acts as a low energy effective Hamiltonian:

$$\begin{aligned} H_{\text{eff},0} &= \sum_{R \in \mathcal{A}} K \left( (S_R^+)^3 s_{R,1}^- s_{R,2}^- s_{R,3}^- + (S_R^-)^3 s_{R,1}^+ s_{R,2}^+ s_{R,3}^+ \right), \\ K &\sim \frac{J^3}{D^2}. \end{aligned} \quad (25)$$

Notice that at low energy, only terms with  $(S^+)^3$  and  $(S^-)^3$  can survive, while terms like  $(S_R^+)^3 (s_{R,1}^-)^2 s_{R,2}^-$  must vanish because  $(s^-)^2 = 0$  for spin-1/2 operator  $s^\pm$ .

Two other effects need to be discussed: (1) at the second order perturbation of  $J/D$ , the  $J_2$  term in Eq. 24 will be renormalized, and shifted by  $\sim J^2/D$ . We assume that the renormalized  $J_2$  is very small and negligible. (2) The 3rd order perturbation of  $J_1$  will generate a new term

$$H'_{\text{eff}} \sim \sum_{R, R' \in \mathcal{A}} \frac{J_1^3}{D^2} \left( (S_R^+)^3 (S_{R'}^-)^3 + \text{h.c.} \right) \quad (26)$$

Now, if we combine Eq. 25 and Eq. 26 together and use the standard spin-boson mapping:  $S_R^+ \sim \exp(i\theta_R)$  and  $s_{R,b}^+ \sim \exp(i\theta_{R,b})$ , the entire low energy effective Hamiltonian is mapped to

$$H_{\text{eff}} = \sum_{R \in \mathcal{A}} -t \cos(3\theta_R - \theta_{R,1} - \theta_{R,2} - \theta_{R,3})$$

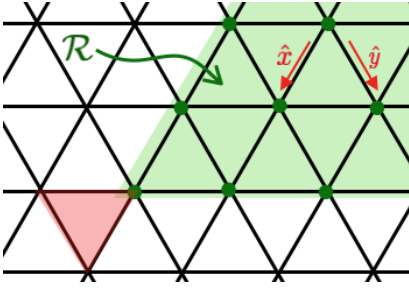


FIG. 4: No excitations are created at the upward-facing triangles that border an edge of region  $\mathcal{R}$ , as shown.

$$- \sum_{R,R' \in \mathcal{A}} t' \cos(3\theta_R - 3\theta_{R'}). \quad (27)$$

Due to the  $t'$  term, at zero temperature  $3\theta_R$  will order on  $\mathcal{A}$  sublattice. If we replace  $3\theta_R$  with its expectation value, then Eq. 27 reduces to Eq. 2 on a triangular lattice, which corresponds to the sublattice  $\mathcal{B}$  of the original honeycomb lattice.

When we map the spin model to a boson rotor model, there is one extra subtlety that the boson number takes half-integer, rather than integer values. This to some extent complicates the analysis of the phase where  $\theta$  is disordered, due to the extra degeneracy arising from  $S^z$ .

### Pascal's Triangle Symmetry of the U(1) Parent Model

In this section, we establish the presence of a generalized fractal symmetry of the U(1) parent Hamiltonian (2) given an appropriate set of boundary conditions. When these boundary conditions are not satisfied, we establish that these approximate symmetries give rise to low-energy modes. Furthermore, we show that the  $Z_p$  generalization of the Sierpinski triangle model exhibits a ground-state degeneracy of  $D = p^{L-1}$  on an  $L \times L$  system with periodic boundary conditions, when  $L = p^k - 1$ .

For the U(1) parent Hamiltonian, starting with the lowest-energy configuration with  $\theta_i = 0$  everywhere (with energy  $E_0$ ), we may perform the transformation

$$\theta_i \rightarrow \theta_i + \frac{2\pi}{p} (-1)^{i_x+i_y} \begin{pmatrix} i_x + i_y \\ i_y \end{pmatrix} \quad (28)$$

within a region  $\mathcal{R}_{(0,0)}$  which consists of the points contained within an equilateral triangle of side-length  $p^k$  with the top of the triangle at the origin  $(i_x, i_y) = (0, 0)$ , i.e.

$$\mathcal{R}_{(0,0)} \equiv \{(i_x, i_y) \mid 0 \leq i_y \leq i_x \text{ and } i_x + i_y \in [0, p^k - 1]\}$$

where  $p$  is a *prime* number and  $k \geq 0$  is an integer. This transformation creates three excitations – downward-facing triangles at which  $\theta_i + \theta_{i+\hat{x}} + \theta_{i+\hat{x}-\hat{y}} \neq 0 \pmod{2\pi}$  – at each corner of the triangular region  $\mathcal{R}$ . The energy of the final state is

$$E_0 + 3t \left[ 1 - \cos\left(\frac{2\pi}{p}\right) \right] \quad (29)$$

We may demonstrate this as follows. The transformation (28) creates an excitation at the downward-facing triangle whose bottom corner sits at the origin since  $\theta_{-\hat{x}} + \theta_0 + \theta_{-\hat{y}} \rightarrow \theta_{-\hat{x}} + \theta_0 + \theta_{-\hat{y}} + (2\pi/p)$  under the transformation (28). Identical excitations are created at the two downward-facing triangles at the two other corners of  $\mathcal{R}_{(0,0)}$ .

We now demonstrate that the transformation (28) acts trivially everywhere away from the corners of  $\mathcal{R}_{(0,0)}$ . First, this transformation does not create any excitations at downward-facing triangles that are contained entirely within the region  $\mathcal{R}_{(0,0)}$ , i.e.  $\theta_i + \theta_{i+\hat{x}} + \theta_{i+\hat{x}-\hat{y}}$  is unchanged by the transformation for any triangle for which  $i$ ,  $i+\hat{x}$ , and  $i+\hat{x}-\hat{y}$  are contained entirely in  $\mathcal{R}_{(0,0)}$ . This can be verified explicitly by applying the transformation (28).

Now, we may consider downward-facing triangles that border an edge of  $\mathcal{R}_{(0,0)}$ . Consider downward-facing triangles that border the bottom of region  $\mathcal{R}_{(0,0)}$ , as shown in Fig. 4. The vertices of these triangles are located at points  $(i, i+\hat{x}, i+\hat{x}-\hat{y})$  for which  $i, i+\hat{x}-\hat{y} \in \mathcal{R}$  while  $i+\hat{x} \notin \mathcal{R}$ . It can be seen that for these downward facing triangles, the transformation (28) leads to the shift

$$\theta_i + \theta_{i+\hat{x}} + \theta_{i+\hat{x}-\hat{y}} \rightarrow \theta_i + \theta_{i+\hat{x}} + \theta_{i+\hat{x}-\hat{y}} + \frac{2\pi}{p} (-1)^{i_x+i_y} \left[ \begin{pmatrix} i_x + i_y \\ i_y \end{pmatrix} + \begin{pmatrix} i_x + i_y \\ i_y - 1 \end{pmatrix} \right] = \theta_i + \theta_{i+\hat{x}} + \theta_{i+\hat{x}-\hat{y}} + \frac{2\pi}{p} \begin{pmatrix} p^k \\ i_y \end{pmatrix}$$

In the last equality, we've used the fact that  $i_x + i_y =$

$p^k - 1$  for the downward-facing triangles bordering the

bottom edge of  $\mathcal{R}_{(0,0)}$ . We now observe that

$$\binom{p^k}{i_y} = 0 \pmod{p} \quad (30)$$

for any  $1 \leq i_y \leq p^k - 1$ . This may be proven by observing that

$$i_y \binom{p^k}{i_y} = p^k \binom{p^k - 1}{i_y - 1} \quad (31)$$

The prime  $p$  divides the right-hand-side of (31) at least  $k$  times. Furthermore, since  $1 \leq i_y \leq p^k - 1$ ,  $p$  divides  $i_y$  at most  $k - 1$  times. As a result,  $p$  must divide  $\binom{p^k}{i_y}$  at least once, which completes the proof. From this, we conclude that  $\theta_i + \theta_{i+\hat{x}} + \theta_{i+\hat{x}-\hat{y}}$  is shifted by an integer multiple of  $2\pi$  for downward-facing triangles that border the bottom edge of  $\mathcal{R}_{(0,0)}$ . Therefore, when starting from the state with  $\theta_i = 0$  everywhere, only three excitations are created by the transformation (28) which lie at the corners of  $\mathcal{R}_{(0,0)}$ , and the energy cost of the final state is indeed given by (29).

We conclude by determining the ground-state degeneracy of the  $Z_p$  models on an  $L \times L$  triangular lattice with periodic boundary conditions, for particular values of  $L$ . First, the previous discussion of the Pascal's symmetry implies that if we start from a configuration with  $\theta_i = 0$  everywhere and perform a symmetry transformation over the region  $\mathcal{R}_{(0,0)}$ , then the configuration of  $\theta_i$  along the row defined by  $i_x + i_y = p^k - 1$  of the lattice is given by

$$\theta_i \pmod{2\pi} = \begin{cases} (-1)^{i_y} \frac{2\pi}{p} & i_y \in [0, p^k - 1] \\ 0 & \text{otherwise} \end{cases}$$

Now consider another symmetry transformation along the region  $\mathcal{R}_{(-1,1)}$ , i.e. along the equilateral triangle of side length  $p^k$  whose top vertex lies at the site  $(i_x, i_y) = (-1, 1)$ . Superposing this transformation with the previous transformation along  $\mathcal{R}_{(0,0)}$ , we find that along the row  $i_x + i_y = p^k - 1$ , that

$$\theta_i \pmod{2\pi} = \begin{cases} \frac{2\pi}{p} & i_y = 0 \text{ or } p^k \\ 0 & \text{otherwise} \end{cases} \quad (32)$$

If we now impose periodic boundary conditions so that  $(i_x, i_y) \sim (i_x + L, i_y) \sim (i_x, i_y + L)$  where  $L = p^k - 1$ , we observe that the symmetry transformations along  $\mathcal{R}_{(0,0)}$  and  $\mathcal{R}_{(-1,1)}$  have generated a new ground-state of the system, since the row  $i_x + i_y = p^k - 1$  is now identified with row  $i_x + i_y = 0$ , and the configuration (32) is precisely the configuration of  $\theta_i$  along the first row  $i_x + i_y = 0$ .

By applying additional ‘‘pairs’’ of these symmetry transformations (e.g. along  $\mathcal{R}_{(i_x, -i_x)}$  and  $\mathcal{R}_{(i'_x, -i'_x)}$ ), we may generate other ground-state configurations. Each unique ground-state corresponds to a unique configuration of  $\theta_i = \frac{2\pi}{p} m_i$  for  $m_i \in [0, \dots, p - 1]$  at each site along the row  $i_x + i_y = 0$ . Not all of these  $p^L$  configurations can be reached by starting with the ground-state with  $\theta_i = 0$  everywhere and applying the fractal symmetry transformation in pairs. It is clear, however, that by continuing to apply these symmetry transformations in pairs, any configuration of  $\theta_i$  along the row  $i_x + i_y = 0$  can be reached for which

$$\sum_{i|i_x+i_y=0} (-1)^{i_y} m_i = 0 \pmod{p} \quad (33)$$

There are precisely  $p^{L-1}$  such configurations. We conclude that the ground-state degeneracy of the  $Z_p$  model is  $p^{L-1}$  on an  $L \times L$  lattice with periodic boundary conditions when  $L = p^k - 1$ .

### Three-point correlation of the $Z_p$ and $Z_N$ models

Starting from the classical  $Z_p$  Pascal's triangle models in Eq. 6, since the  $Z_p$  clock degrees of freedom are primitive  $p$ -roots of unity for which  $\sigma^\dagger = \sigma^{p-n}$ ,  $\text{Re } \sigma = \text{Re } \sigma^{p-n}$ ,  $\text{Im } \sigma = -\text{Im } \sigma^{p-n}$  and likewise for the dual  $\tau$ -variables. As a result, for the partition function of a single  $\tau$ -variable  $Z_1 = \sum_{n=0}^{p-1} e^{\beta t \cos(\frac{2\pi n}{p})}$ :

$$\begin{aligned} \langle \text{Im } \tau^m \rangle &= \frac{1}{Z_1} \sum_{n=0}^{p-1} \sin\left(\frac{2\pi mn}{p}\right) e^{\beta t \cos(\frac{2\pi n}{p})}, \\ &= 0; \end{aligned} \quad (34)$$

$$\begin{aligned} \langle \text{Re } \tau^m \rangle &= \frac{1}{Z_1} \sum_{n=0}^{p-1} \cos\left(\frac{2\pi mn}{p}\right) e^{\beta t \cos(\frac{2\pi n}{p})}, \\ &= \frac{1}{Z_1} \sum_{n=0}^{p-1} \cos\left(\frac{2\pi m(p-n)}{p}\right) e^{\beta t \cos(\frac{2\pi n}{p})}, \\ &= \langle \text{Re } (\tau^m)^\dagger \rangle. \end{aligned} \quad (35)$$

As a consequence,  $\langle \tau^m \rangle = \langle (\tau^m)^\dagger \rangle$ . In the dual representation, the three-point correlation function factors since each  $\tau$  is statistically independent

$$\begin{aligned} \mathcal{C}_3(r = p^k) &= \langle \sigma_{0,0} \sigma_{r,0} \sigma_{0,r} \rangle, \\ &= \langle \text{product of } \tau^m \text{ in Pascal's triangle} \rangle, \\ &= \text{product of } \langle \tau^m \rangle \text{ in Pascal's triangle}, \\ &= \prod_{m=1}^{\frac{p-1}{2}} \langle \tau^m \rangle^{N_{m,p-m}(k)}, \end{aligned} \quad (36)$$

where  $N_{m,p-m}(k)$  is the number of times  $m$  and  $p - m$  appear in the Pascal's triangle modulo  $p$  of length  $p^k - 1$ .



Note that the staggering of  $\tau$ -variables in the representation of  $\sigma$  is inconsequential for the calculation of the three-point correlation as  $\langle \tau^m \rangle = \langle (\tau^m)^\dagger \rangle$ .

As a result, computing the three-point correlation function reduces to counting the number of times each unique entry in a Pascal's triangle modulo  $p$  appears. Since the elements of a Pascal's triangle modulo  $p$  are binomial coefficients  $\binom{j}{i} \bmod p$ , one may in principle calculate  $N_{m,p-m}(k)$  by brute force according to

$$N_{m,p-m}(k) = \sum_{i \leq j} \sum_{j=0}^{p^k-1} \delta \left( m, \binom{j}{i} \bmod p \right) + \sum_{i \leq j} \sum_{j=0}^{p^k-1} \delta \left( p-m, \binom{j}{i} \bmod p \right). \quad (37)$$

However, this is neither efficient analytically nor numerically, even at small  $p$ . It is instead desirable to derive recurrence relations that can be solved assuming initial conditions  $N_{m,p-m}(1)$  are provided which can be computed according to Eq. 37 with  $k = 1$ . In order to derive such recurrence relations, we can make use that for  $\cos(m\phi)$ ,  $m = 1, \dots, \frac{p-1}{2}$  such that

$$\cos(m\phi) = \cos(qn\phi) \Leftrightarrow \begin{cases} m = qn \bmod p \\ m = q(p-n) \bmod p \end{cases}. \quad (38)$$

This implies that  $\langle \tau^m \rangle = \langle \tau^{qn} \rangle$  where  $q = q(m, n)$  is the smallest element of  $Z_p$  for which one of the two equations in Eq. 38 is solved. If we consider an arbitrary Pascal's triangle modulo  $p$  of length  $p^k - 1$ , this triangle is self-similar and can be constructed by tiling the same Pascal's triangle of length  $p^{k-1} - 1$  according to the Pascal's triangle of length  $p - 1$ . The number of  $\langle \tau^n \rangle$  which become  $\langle \tau^m \rangle$  upon tiling is  $N_{q(m,n), p-q(m,n)}(1)$ . As a result, we arrive at a set of  $\frac{p-1}{2}$  coupled recurrence relations

$$N_{m,p-m}(k) = \sum_{n=1}^{\frac{p-1}{2}} N_{q(m,n), p-q(m,n)}(1) N_{n,p-n}(k-1) \quad (39)$$

For small  $p$ ,  $N_{m,p-m}(1)$  can be calculated and these recurrence relations can be solved without the use of numerics. For example, for the  $p = 5$  model

$$q = \begin{bmatrix} 1 & 2 \\ 2 & 1 \end{bmatrix}.$$

One can compute the initial conditions by hand from Eq. 37 to find  $N_{1,4}(1) = 12$  and  $N_{2,3}(1) = 3$ , yielding coupled recurrence relations

$$N_{1,4}(k) = 12N_{1,4}(k-1) + 3N_{2,3}(k-1), \quad (40)$$

$$N_{2,3}(k) = 12N_{2,3}(k-1) + 3N_{1,4}(k-1). \quad (41)$$

This can be solved again using the initial conditions to recover

$$N_{1,4}(k) = \frac{3^{k-1}}{10} (3 \times 5^{k+1} + 5 \times 3^{k+1}),$$

$$N_{2,3}(k) = \frac{3^{k-1}}{10} (3 \times 5^{k+1} - 5 \times 3^{k+1}).$$

One can verify that  $N_{1,4}(k) + N_{2,3}(k)$  must be the area of the fractal of length  $p^k - 1$ ,  $N_{1,4}(k) + N_{2,3}(k) = 15^k = 5^k \times \frac{\ln 15}{\ln 5} = 5^k \times d_H$ . The three-point correlation can now be computed as

$$\begin{aligned} \mathcal{C}_3(r = 5^k) &= \langle \tau \rangle^{N_{1,4}(k)} \langle \tau^2 \rangle^{N_{2,3}(k)}, \\ &= \left( \frac{1}{Z_1} \sum_{n=0}^{p-1} \cos \left( \frac{2\pi n}{p} \right) e^{\beta t \cos \left( \frac{2\pi n}{p} \right)} \right)^{N_{1,4}(k)} \\ &\times \left( \frac{1}{Z_1} \sum_{n=0}^{p-1} \cos \left( \frac{4\pi n}{p} \right) e^{\beta t \cos \left( \frac{2\pi n}{p} \right)} \right)^{N_{2,3}(k)} \\ &\approx \left( \frac{e^{\beta t} + 0.62e^{0.31\beta t} - 1.62e^{-0.81\beta t}}{e^{\beta t} + 2e^{0.31\beta t} + 2e^{-0.81\beta t}} \right)^{N_{1,4}(k)} \\ &\times \left( \frac{e^{\beta t} - 1.62e^{0.31\beta t} + 0.62e^{-0.81\beta t}}{e^{\beta t} + 2e^{0.31\beta t} + 2e^{-0.81\beta t}} \right)^{N_{2,3}(k)} \quad (42) \end{aligned}$$

For sufficiently large distances,  $\mathcal{C}_3(r = 5^k) \sim e^{-\alpha' r^\gamma}$  where  $\gamma$  is an exponent that is larger than  $d_H$ , due to the decay of  $\langle \tau^2 \rangle$  being stronger than  $\langle \tau \rangle$ . As a comparison, the three-point correlation in the  $Z_5$  model decays much faster than the three-point correlation of the Sierpinski-triangle model and the  $Z_3$  Pascal's triangle model.

The multiple fractal symmetries of the  $Z_N$  models has important consequences for the behavior of the three-point correlations as well. All of the  $Z_N$  models retain the same dual description, and  $\sigma$  can be represented as an infinite staggered product of dual  $\tau$ -variables on a Pascal's triangle modulo  $N$  in the thermodynamic limit. However, since  $N$  is composite, this Pascal's triangle is not a fractal and hence there is no product of three  $\sigma$ 's that has compact support causing  $\mathcal{C}_3(r)$  to vanish. Instead, for each unique prime divisor  $p$  of  $N$  for which  $qp = N$ ,  $\sigma^q$  can be represented as an infinite staggered product of  $\tau^q$  in the shape of a Pascal's triangle modulo  $p$ . Therefore,  $\mathcal{C}_3^q(r) = \langle \sigma_{0,0}^q \sigma_{r,0}^q \sigma_{0,r}^q \rangle$  is non-vanishing when  $r = p^k$ . Using  $Z_{N=6}$  as an example again,  $\mathcal{C}_3^3 = \langle \sigma_{0,0}^3 \sigma_{r,0}^3 \sigma_{0,r}^3 \rangle$  characterizes SSB of the  $Z_2$  fractal symmetry while  $\mathcal{C}_3^2 = \langle \sigma_{0,0}^2 \sigma_{r,0}^2 \sigma_{0,r}^2 \rangle$  characterizes SSB of the  $Z_3$  fractal symmetry. Note that if  $N$  is taken to be prime, since the only prime-factor of  $N$  is itself, these results reduce down to those of the  $Z_p$  models and  $\langle \sigma_{0,0} \sigma_{r,0} \sigma_{0,r} \rangle$  is ordered.

### A related model with stable $\sqrt{3} \times \sqrt{3}$ order

We consider a model directly related to Eq. 14, but instead is stable against the inclusion of quantum fluctu-

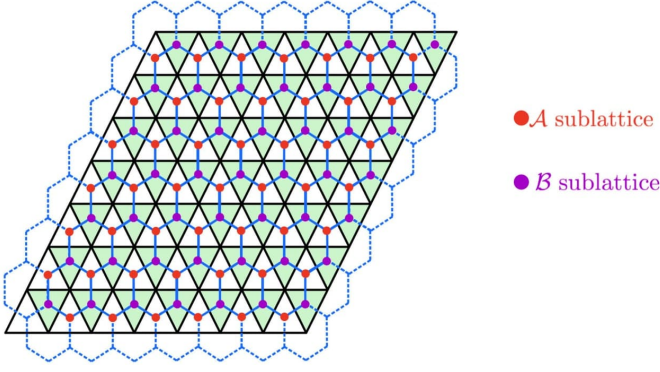


FIG. 5: The dual honeycomb lattice where Eq. 46 is defined on. Each vertex of the honeycomb lattice coincides with either a downward or upward facing plaquette of the original triangular lattice.

ations. In the U(1) parent model, the Pascal’s triangle fractal symmetries only exist because a single orientation of triangular plaquettes is being summed over. If we include the sum over three-boson interactions on upward facing plaquettes as well, the model becomes

$$H = \sum_{\nabla, \Delta} -t \cos(\theta_1 + \theta_2 + \theta_3) + \sum_j \frac{U}{2} n_j^2. \quad (43)$$

While this model does not have the Pascal’s triangle fractal symmetries of Eq. 14, it still retains the global  $U(1)_1 \times U(1)_2$  symmetry in Eq. 3 and hence the ground state of this model at small  $U$  will still have the  $\sqrt{3} \times \sqrt{3}$  order. In this case, unlike Eq. 14, the boson ordered phase will actually be stable against quantum fluctuations. This can be seen by analyzing the dual of Eq. 43. Now, the dual variables are defined on the sites  $\bar{i}$  of the dual honeycomb lattice (Fig. 5):

$$\begin{aligned} \theta_1 + \theta_2 + \theta_3 &= \phi_{\bar{i}}, \quad \text{site } 1, 2, 3 \text{ around } \bar{i}; \\ n_j &= \sum_{\bar{i}} \Psi_{\bar{i}}, \quad \bar{i} = 1, \dots, 6 \text{ around } j. \end{aligned} \quad (44)$$

The dual variable is subject to a local gauge constraint around each site  $j$ :

$$\sum_{\bar{i} \text{ around } j} (-1)^{\bar{i}} \phi_{\bar{i}} = 0 \pmod{2\pi}. \quad (45)$$

Again,  $\phi_{\bar{i}}$  are compact variables, while  $\Psi_{\bar{i}}$  takes discrete values. The dual Hamiltonian of Eq. 43 reads [32]

$$H_d = \sum_{\bar{j}} -t \cos(\phi_{\bar{j}}) + \sum_j \frac{U}{2} \left( \sum_{\bar{i} \text{ around } j} \Psi_{\bar{i}} \right)^2. \quad (46)$$

The key difference from the model considered in the main text is that, this dual model Eq. 46 has a gauge symmetry, i.e. the dual Hamiltonian is invariant under the following local gauge transformation:

$$\Psi_{\bar{i}} \rightarrow \Psi_{\bar{i}} + (-1)^{\bar{i}} \epsilon_j, \quad \bar{i} \text{ around } j, \quad (47)$$

where  $\epsilon_j$  is an arbitrary integer-valued function on the original triangular lattice  $j$ .

Now we can again replace  $\Psi_{\bar{i}}$  by continuous variables, and the constraint that  $\Psi$  takes discrete values will be enforced through “vertex operators” such as  $\cos(2\pi\Psi)$ . If we ignore these vertex operators, the Lagrangian of the Gaussian theory of Eq. 46 reads:

$$\mathcal{L}_d = \sum_{\bar{i}} \frac{1}{2t} (\partial_\tau \Psi_{\bar{i}})^2 + \sum_j \frac{U}{2} \left( \sum_{\bar{i} \text{ around } j} \Psi_{\bar{i}} \right)^2. \quad (48)$$

This Gaussian theory has a continuous gauge symmetry, which corresponds to allowing  $\epsilon_j$  to take arbitrary continuous values in Eq. 47. Then, the Gaussian fixed point of Eq. 48 is stable against weak vertex operators, since the vertex operators break the continuous gauge symmetry of the Gaussian theory Eq. 48.